TB68

19th International Symposium of Ballistics, 7–11 May 2001, Interlaken, Switzerland

TAYLOR IMPACT EXPERIMENTS OF ELECTRIFIED COPPER AND ALUMINUM CYLINDERS

Peter Bartkowski, Michael Keele, William Bruchey

U.S. Army Research Laboratory, Aberdeen Proving Ground, MD 21005 USA

In development of an Electro-Magnetic (EM) Armor system for combat vehicles, there is a lack of information on the dynamic EM-Mechanical effects on materials to support modeling and simulation efforts. In an effort to understand the coupled EM-Mechanical effects, a series of modified Taylor Impact experiments were designed to measure the dynamic response of OFHC Copper and 6061-T6 Aluminum cylinders subjected to simultaneous mechanical and electrical loads. The cylinders were fired up to 300 m/s from a high-pressure gas gun through a negatively charged electrode collar, striking a positively charged anvil; creating an electrical discharge through the cylinder as plastic deformation occurred. The levels of electrical energy delivered to the test cylinders were varied for a given range of impact velocities so as to characterize the plastic deformation of each cylinder material as a function of electrical energy delivered. The experimental results are to be analyzed by hand-shaking a well established ohmic heating model with a conventional Taylor Impact analytical model. The ohmic heating model is two-dimensional and treats current conduction and heat transport through a moving, axi-symmetric conductor. Solutions are obtained to the coupled, nonlinear Maxwell and energy transport equations. The experimental baseline results are presented.

INTRODUCTION

The study of plastic deformation using the impact of cylindrical rods on rigid anvils was pioneered by Taylor [1]. Taylor developed a simple model to relate the resulting rod profile after the experiment to the dynamic yield stress in the material.

Subsequent investigators [2–7] have improved upon Taylor's work with more accurate models of the plastic deformation. Current state of the art techniques use sophisticated numerical simulations to analyze the dynamic deformation in addition to the final cylinder profile.

Experiments have also been conducted at elevated temperatures to determine the change in dynamic yield strength with temperature.

This work takes that effort one step further by determining the dynamic material properties due to Electro-magnetic (EM) effects. Large current discharges are used to rapidly heat the rod and generate EM fields as deformation is occurring. State of the art X-ray radiography and high speed framing cameras are employed to probe the stages of material deformation while electrical energy is measured during the discharge.

PREVIOUS WORK

W. H. Gust performed reverse Taylor experiments on a variety of materials at elevated temperatures [8]. The tests Gust performed consisted of using a gas gun to fire a target at a stationary rod that was heated to an elevated temperature (Fig. 1). The stationary rods were 6 mm diameter and 30 mm long. The flying target consisted of two layers. The first being a 12 mm thick Alumina disc 25 mm in diameter backed by a similar diameter, 15 mm thick aluminum disc.

The rods were heated slowly to temperatures of 730° K and 1235° K, using infrared radiation prior to the launch of the target discs. A soft recovery technique was employed to recover the rods without further deformation.

A series of baseline tests were conducted by Gust at room temperature to compare the reverse impact tests to the traditional rod launched results. These tests yielded the same experimental results, validating the reverse impact technique. These tests are used to validate our experimental technique as well.

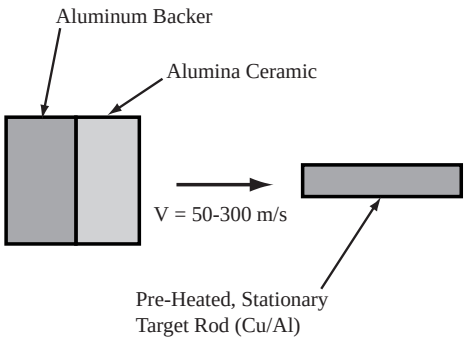

Figure 1. Gust's experimental configuration.

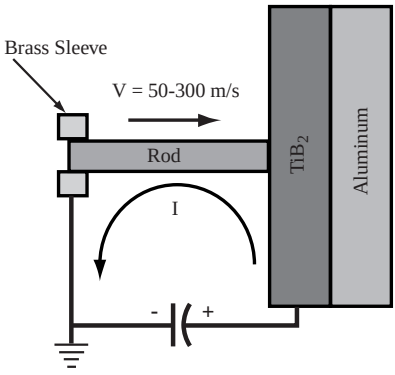

Figure 2. Current exp. configuration.

EXPERIMENTAL CONFIGURATION

Our experimental configuration consists of the more traditional technique of launching rods with velocities between 50 – 300 m/s at a stationary target. Velocity is varied by changing the charge pressure in the air gun's reservoir. The baseline (unelectrified)

tests conducted used OFHC Copper and 6061 Aluminum rods impacting a two layer target consisting of 12 mm thick Alumina backed by 12 mm thick aluminum. The target tiles were nominally 100 mm square.

The electrified tests will be similar but use either hardened steel or TiB_2 ceramic instead of Alumina to provide an electrically conductive "hot" target. A brass collar insulated from the end of the gun barrel will provide a ground path for the electricity. The rod will fire through the ground sleeve and impact the ihhotlh target, completing the electrical circuit, creating an electrical discharge through the rod as impact and subsequent rod deformation is occurring.

Electrical energy will be delivered from a capacitor bank consisting of up to 10, 200 uf capacitors rated at 22 KV maximum voltage. Current feed to the rod is symmetrical via "stop sign" electrode plates to eliminate any net force vector acting on the rod due to the created magnetic field.

DIAGNOSTICS

A suite of diagnostics will be employed to determine the effects of the EM discharge on the rod during and after the experiment. Rod velocity is determined by a recording the time interval between a set of pre-measured laser breaks at the end of the gun barrel.

A Rogowski coil connected to a 2 GSa/s digital oscilloscope measures the electrical discharge by recording the charge vs. time. Numerically integrating this signal yields the current vs. time the rod is subjected to during the experiment.

Flash X-ray radiography and high speed digital framing is used to observe the change in rod profile as deformation occurs. The flash X-rays consist of 3 overhead and one orthogonal pulser. This allows for 4 images to be recorded as deformation occurs. Similarly, a high speed digital framing camera is also employed to record "snap shots" during the deformation process.

The final rod length and axial profile is determined after recovery from the experiment. Final rod length is measured to ± 0.025 mm. An image analysis software package is used to measure an axial profile of the rods from the images acquired during deformation as well as after recovery for comparison with numerical simulations.

MATERIALS

The materials of interest for these experiments are: OFHC Copper, 6061 Aluminum, Tantalum, Molybdenum, and 316 Stainless Steel. Baseline tests were conducted on the Copper and Aluminum to validate the experimental setup and operation.

BASELINE (UN-ELECTRIFIED) TESTS

Experimental Results

A series of baseline tests were conducted on OFHC Copper and 6061 Aluminum to verify our experimental technique. The first tests conducted, used 6 mm diameter x 75 mm long rods. Figures 3 & 4 show the results from the experiments on the copper and aluminum respectively. These tests were conducted at impact velocities nominally 155 m/s and 300 m/s. It is apparent from the images, that buckling occurred during deformation process.

The next sequence of tests used 6 mm diameter x 50 mm long rods. These tests yielded virtually no buckling in either the copper or the aluminum (Fig. 5 & 6). It is important to keep these rods as long as possible for the electrified tests. This allows longer standoff between electrode plates to help prevent accidental discharge. A length of 50 mm provides a good compromise between buckling and standoff and will be used for the future tests. A summary of the baseline tests conducted on OFHC copper and 6061 aluminum is given in Table 1.

Figure 3. 75 mm OFHC Cu Rods.

Figure 4. 75 mm 6061 Al Rods.

One traditional method of comparing Taylor experiments is the ratio of final rod length to original length. In addition to the rod length, we have measured the rod tip diameter to compare the final to initial tip diameter ratio. Deformation of the tip however is not perfectly symetrical radially. The tip diameter is reported as a range between the minimum and maximum diameter measured. A few of the experiments resulted in mushrooming of the rod tip where diameter can not be adequately quantified, these are noted in Table 1.

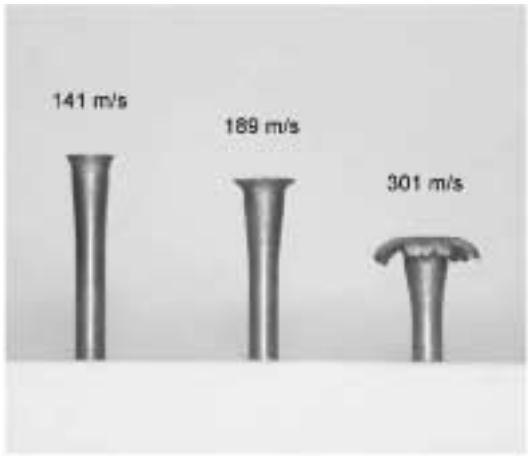

Figure 5. 50 mm OFHC Cu rods.

Figure 6. 50 mm 6061 Aluminum rods.

For comparison, the length ratio data in Table 1 is plotted along with Gust's ambient temperature data in Fig. 7. Our baseline tests on 6061 Aluminum show excellent agreement with Gust's tests at room temperature. One thing to note is that our OFHC copper results do not match the annealed copper results published by Gust. They do however, match the initial un-annealed copper validation tests performed by Gust (used in Fig. 7). These test results validate our experimental setup and operation.

The measured maximum and minimum final rod tip diameter ratios are plotted in Fig. 8 are clearly more variable than the measured residual lengths.

Yield Stress Calculation

Taylor's analysis [1] of the plastic deformation of a rod impacting a rigid anvil used the following formulation which makes several assumptions. First, the rate of decrease in rod length is proportional to impact velocity. Second, the material flows perfectly plastically and that the rod decelerates as a rigid body:

TABLE 1. Baseline experimental data summary.

Exp #	Rod Material	Rod Dia. (mm)	Rod Lo (mm)	Vel. (m/s)	Rod Lf (mm)	Lf/Lo	Tip Dia (mm)	Df/Do
13	Al 6061	6.25	74.75	306.0	57.66 *	0.771	14.02-14.45	2.244-2.313
14	Al 6061	6.25	74.83	306.5	57.58 *	0.770	12.17-12.95	1.947-2.073
18	Al 6061	6.27	74.93	166.7	68.83 *	0.919	7.14-8.03	1.138-1.279
19	Al 6061	6.27	74.90	159.0	69.29 *	0.925	7.70-7.82	1.227-1.247
20	Al 6061	6.30	49.99	156.3	46.36	0.927	8.10-8.28	1.286-1.315
21	Al 6061	6.30	49.91	194.0	44.60	0.894	8.51-8.81	1.351-1.399
22	Al 6061	6.30	49.99	311.0	38.48	0.770	#	
15	Cu OFHC	6.27	74.93	328.0	38.48 *	0.514	#	
16	Cu OFHC	6.30	74.96	130.0	65.28 *	0.871	9.17-9.45	1.456-1.500
17	Cu OFHC	6.30	74.96	152.0	61.85 *	0.825	10.74-11.05	1.706-1.754
23	Cu OFHC	6.30	49.94	156.6	42.95	0.860	10.26-10.49	1.629-1.665
24	Cu OFHC	6.30	50.01	140.5	42.88	0.857	10.03-10.19	1.593-1.617
25	Cu OFHC	6.30	50.01	301.0	25.68	0.513	#	
26	Cu OFHC	6.30	49.96	189.0	37.97	0.760	13.08-13.21	2.077-2.097
27	Cu OFHC	6.30	49.99	186.3	37.97 †	0.760	13.16-13.39	2.089-2.125
28	Cu OFHC	6.30	49.99	190.3	38.46 †	0.769	12.52-12.83	1.988-2.036

* denotes buckling in rod occurred; † denotes epoxy between targets; # denotes mushrooming of rod tip

$$\frac{L_f}{L_0} = \exp\left(\frac{\rho_0 U^2}{2\sigma_{yd}}\right) \qquad (1)$$

Where: L_f = final length
L_0 = initial length
ρ_0 = density
U = impact velocity
σ_{yd} = yield stress

As noted by Wilkins & Guinan, the above analysis assumes the plastic wave front remains at the rigid boundary while infact, it travels down the rod. While the above ibscaling lawla is valid, a correction can be made to account for the movement of the plastic wave front from the rigid boundary.

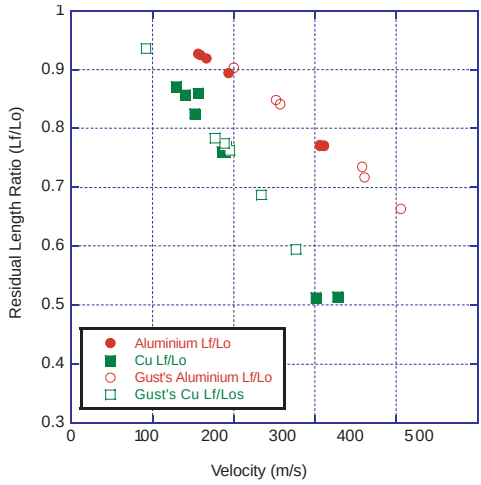

Figure 7. Final lenght ratio.

Wilkins & Guinan noticed that in their simulations, the plastic wave front appeared to move to an approximately fixed position (h) away from the rigid boundary that was proportional to original rod length (L_0). Using this observation they derived the following relationship between the residual length of the rod and the yield stress:

$$\frac{L_f}{L_0} = \left(1 - \frac{h}{L_0}\right)\exp\left(-\frac{\rho_0 U^2}{2\sigma_{yd}}\right) + \frac{h}{L_0} \qquad (2)$$

Where: L_f = final length
L_0 = initial length
h = plastic def. length
ρ_0 = density
U = impact velocity
σ_{yd} = yield stress

Rearranging the above equation and solving for the dynamic yield stress yields:

$$\sigma_{yd} = \frac{-1/2\rho_0 U^2}{\ln\left(\frac{L_f/L_0 - h/L_0}{1 - h/L_0}\right)} \qquad (3)$$

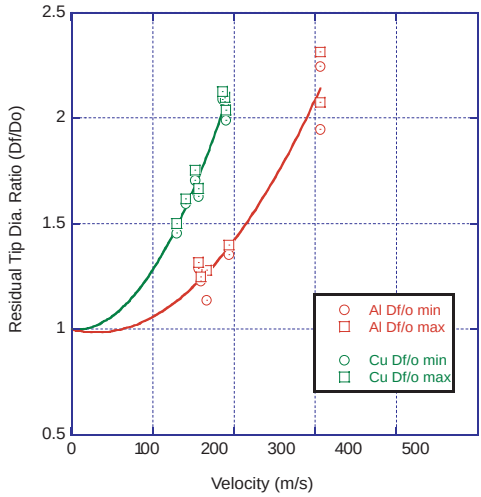

Figure 8. Final tip diameter ratio.

It was also noted that the ratio of final plastic wave position to original rod length was approximately constant at $h/L_o \cong 0.12$ for many materials. Using Eq. 3 and the above assumption on the value of h, the yield stress is calculated for each experiment. The results of the yield stress calculations on the 6061 Aluminum and OFHC Copper are given in Table 2 and can be seen in Fig. 9 below.

Aluminum shows a slight increase of yield stress with impact velocity (strain rate) and compares very well with the value of 420 MPa determined by Wilkins & Guinan (2). As can be seen, the yield stress data for the OFHC Copper is quite scattered and is higher than the 300–390 MPa (89–210 m/s impact velocity) range measured by Wilkins & Guinan (2). This is due to the fact that copper exhibits significant work hardening, creating widely varying yield stresses resulting from variations in manufacturing.

FUTURE WORK

The next step in this project is to identify the pulse characteristics of the capacitor bank and match the rise time of the pulse to the deformation in the rod. We are interested in rise times faster than the deformation process to study the coupling between the EM discharge and mechanical response.

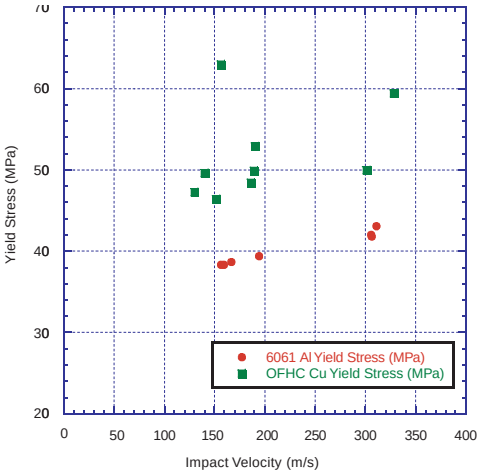

Figure 9. Yield Stress Calculated.

TABLE 2. Yield Stress Calculations.

Exp #	Rod Mat'l	Vel. (m/s)	Lf/Lo	Yield Stress (MPa)
13	Al	306.0	0.771	420
14	Al	306.5	0.770	418
18	Al	166.7	0.919	387
19	Al	159.0	0.925	383
20	Al	156.3	0.927	383
21	Al	194.0	0.894	394
22	Al	311.0	0.770	431
15	Cu	328.0	0.514	594
16	Cu	130.0	0.871	473
17	Cu	152.0	0.825	464
23	Cu	156.6	0.860	630
24	Cu	140.5	0.857	496
25	Cu	301.0	0.513	500
26	Cu	189.0	0.760	499
27	Cu	186.3	0.760	484
28	Cu	190.3	0.769	529

The bulk of the project then consists of conducting the baseline un-electrified and electrified tests on each material. Due to the 3 independent test parameters (material, electrical energy, velocity) the test matrix quickly becomes quite large (5 mat's x 4 Energies x 5 velocities = 100 tests).

The axial profiles measured during and after the tests will then be compared to the numerical simulations in an effort to understand the coupling between the EM discharge and the material response.

REFERENCES

1. Taylor, G.I., *Proceedings of the Royal Society London* **194,** 285–299 (1948)
2. Wilkins, M.L and Guinan, M.W., *Journal of Applied Physics* **44,** 1200–1206 (1973)
3. Woodward, O™Donnel,, and Flockhart, *Journal of Materials Science* **27,** 6411–6415 (1992)
4. Lee, E.H. and Tupper, S.J., *Journal of Applied Mechanics,* 63–70 (March 1954)
5. Meyers, M.A., *Dynamic Behavior of Materials,* J. Wiley, 82–97 (1994)
6. Netherwood, P.H., *U.S. Army BRL Tech Report* No. ARBRL-MR-03137 (1981)
7. Foster, J.C., Maudlin, P.J., and Jones, S.E., *Shock Compression of Condensed Matter,* Seattle, WA 291–294 (1995)
8. Gust, W.H., *Journal of Applied Physics* **53,** 3566–3575 (1982)